

Sluggish news reactions: A combinatorial approach for synchronizing stock jumps*

Nabil Bouamara

Department of Finance, Université catholique de Louvain

Kris Boudt

Department of Economics, Ghent University

Solvay Business School, Vrije Universiteit Brussel

School of Business and Economics, Vrije Universiteit Amsterdam

Sébastien Laurent

Aix Marseille Univ., CNRS, AMSE, Marseille, France

Aix-Marseille Graduate School of Management-IAE

Christopher J. Neely

Research Division, Federal Reserve Bank of St. Louis

September 28, 2023

Abstract

Stock prices often react sluggishly to news, producing gradual jumps and jump delays. Econometricians typically treat these sluggish reactions as microstructure effects and settle for a coarse sampling grid to guard against them. Synchronizing mistimed stock returns on a fine sampling grid allows us to automatically detect noisy jumps and better approximate the true common jumps in related stock prices.

Keywords: Asynchronicity; Cojumps; High-frequency data; Microstructure noise; Realized Covariance; Rearrangement

1 Introduction

Major economic news, such as pre-scheduled announcements, natural disasters or geopolitical conflicts, trigger common jumps in related stock prices (see *e.g.* Li et al., 2017, for some

*We have received helpful comments and suggestions from Andres Algaba, Geert Dhaene, Jean-Yves Gnabo, Roxana Halbleib, Ilze Kalnina, Nathan Lassance, Oliver Linton, André Lucas, Kristien Smedts, Lisa Van den Branden, Steven Vanduffel, Brecht Verbeken and the conference and seminar participants at KU Leuven, Vrije Universiteit Brussel, Vrije Universiteit Amsterdam, the Computational and Financial Econometrics Conference (2021), the Belgian Financial Research Forum (2023), the Quantitative and Financial Econometrics Conference (2023), and the Society of Financial Econometrics Summer School (2023). Nabil Bouamara gratefully acknowledges support from the Flemish Research Foundation (FWO fellowship #11F8419N) and the Platform for Education and Talent (Gustave Boël – Sofina fellowship). Sébastien Laurent has received fundings from the french government under the “France 2030” investment plan managed by the French National Research Agency (reference: ANR-17-EURE-0020 and ANR-21-CE26-0007-01) and from Excellence Initiative of Aix-Marseille University - A*MIDEX.

empirical examples). Statistical tests for these common jumps, or so-called “cojump tests”, implicitly assume that jumps occur simultaneously in relevant assets but, in fact, jumps occur asynchronously in transaction prices. Stock prices can move sluggishly (Bandi et al., 2017), jumps can be gradual (Barndorff-Nielsen et al., 2009) and jumps of less-liquid individual assets typically lag those of the more-liquid market index (Li et al., 2017). Most researchers have dealt with this problem by settling for a coarse sampling grid (see *e.g.*, Barndorff-Nielsen et al., 2009; Bollerslev et al., 2008; Lahaye et al., 2011; Li et al., 2019). Such a coarse grid guards against microstructure effects, the frictions with which actual trades take place, but it is restrictive in that it oversmooths actual changes (see *e.g.*, Ait-Sahalia, 2004).

We offer an alternative strategy which changes the time labels of some financial time series observations on a fine sampling grid to approximately recover the efficient common jump in a basket of stocks. Asynchronous impoundment of news causes the value of a synthetic stock index to deviate from the price of an exchange-traded fund (ETF), even though they consist of the same stocks. Assuming that an ETF price tracks the latent, equilibrium (often called “efficient”) value of a stock index, the spread between the value of a synthetic index and the ETF price measures the sluggishness in news reactions. Combinatoric methods rearrange jumps to minimize the spread and approximately recover the latent efficient price.

To rearrange stock jumps, we extend the pioneering work of Puccetti and Rüschenendorf (2012) and Embrechts et al. (2013) on rearrangements. Their rearrangement algorithm is best known as an actuarial tool to bound portfolio risk, but it can also be applied to other disciplines, such as operations research (see *e.g.*, Boudt et al., 2018). Rearrangements can also synchronize stock jumps and recover the common jump on a fine sampling grid, provided we penalize economically implausible rearrangements. For example, we only allow for a rearrangement of jumps backward in time because we assume that stock prices are sluggish and lag the highly liquid and carefully watched ETF, they do not lead it.

We apply our methods to investigate the reactions of Dow 30 stock prices in event windows around DIA ETF jumps. For example, the Federal Reserve announced rate cuts on September 18, 2007, at 14:15 US Eastern Time, after which markets took up to five minutes to incorporate the Fed’s news into the Dow 30 stock’s prices. Rearrangements synchronize 19 (out of 23) scattered stock jumps with the ETF jump, approximately recovering the common jump in the stocks. This is not a stand-alone event: the rearrangement linear program rearranges stock jumps in 180 cases.

Synchronizing mistimed stock returns improves estimates of the daily realized covariance matrix. Other estimators, like the multivariate realized kernel in Barndorff-Nielsen et al. (2011) or a Cholesky factorization in Boudt et al. (2017), protect against mild market microstructure noise and the Epps (1979) effect, that is, the downward bias in covariance estimates due to asynchronous trading. But rearranging returns protects against the underestimation of jump dependence due to asynchronous jumps and improves the out-of-sample financial performance compared to using raw returns.

We proceed as follows. Section 2 details the synchronization method using a toy example. Section 3 illustrates an empirical example of a rearranged sluggish cojump in the Dow 30 and includes a portfolio allocation exercise. Section 4 concludes.

2 Synchronizing jumps: A combinatorial problem

A salient feature of multivariate high-frequency financial data is the occurrence of non-synchronous trading; it is rare for any two assets to trade simultaneously. This leads to prices at irregularly spaced times, differing across assets. Addressing asynchronicity through

the coordinated collection of multivariate data has been an active area of research in financial econometrics in recent years, see *e.g.*, Barndorff-Nielsen et al. (2011) or Boudt et al. (2017) and the references therein, and the concept of so-called “stale” prices has been integral to covariance estimations since Epps (1979). Nonetheless, the state-of-the-art sampling schemes like refresh-time sampling (Barndorff-Nielsen et al., 2011), are not tailored to price jumps, with asynchronous jumps not necessarily resulting from non-synchronous trading. At times, prices may be “sluggish”; the asset might be trading, but due to various factors, the news might not yet be impounded in the price. To address this problem, we synchronize the timing of multivariate jumps using what we call “Jump Sampling”. This technique refines the detection of high-frequency cojumps and, in turn, the realized covariance matrix.

Figure 1 compares refresh-time sampling to jump sampling in the presence of asynchronous observations and jumps. It draws inspiration from the well-known Figure 1 in Barndorff-Nielsen et al. (2011), illustrating refresh-time in a situation with three assets (without the occurrence of jumps). We expand upon this concept to include scenarios with asynchronous price jumps, focusing on three specific assets: a basket instrument and its two underlying stocks. In each asset’s case, the filled dots indicate the updates in posted prices, and an open dot pinpoints the time at which the price jumps. Vertical dashed lines represent the sampling times generated from the three assets, using the refresh-time sampling approach. For example, the first black dot represents the time it has taken for all three assets to trade. But because asynchronous jumps are not due to (il)liquidity issues, refresh-time sampling does not resolve the asynchronicity inherent in the jumps. As a solution, we introduce a new jump sampling scheme, which rearranges mistimed jumps to occur simultaneously with the ETF jump.

In what follows, we detail how we synchronize stock jumps using combinatorics. We optimally rearrange jumps, penalizing economically implausible rearrangements. A simulated example clarifies the mechanics of the rearrangements.

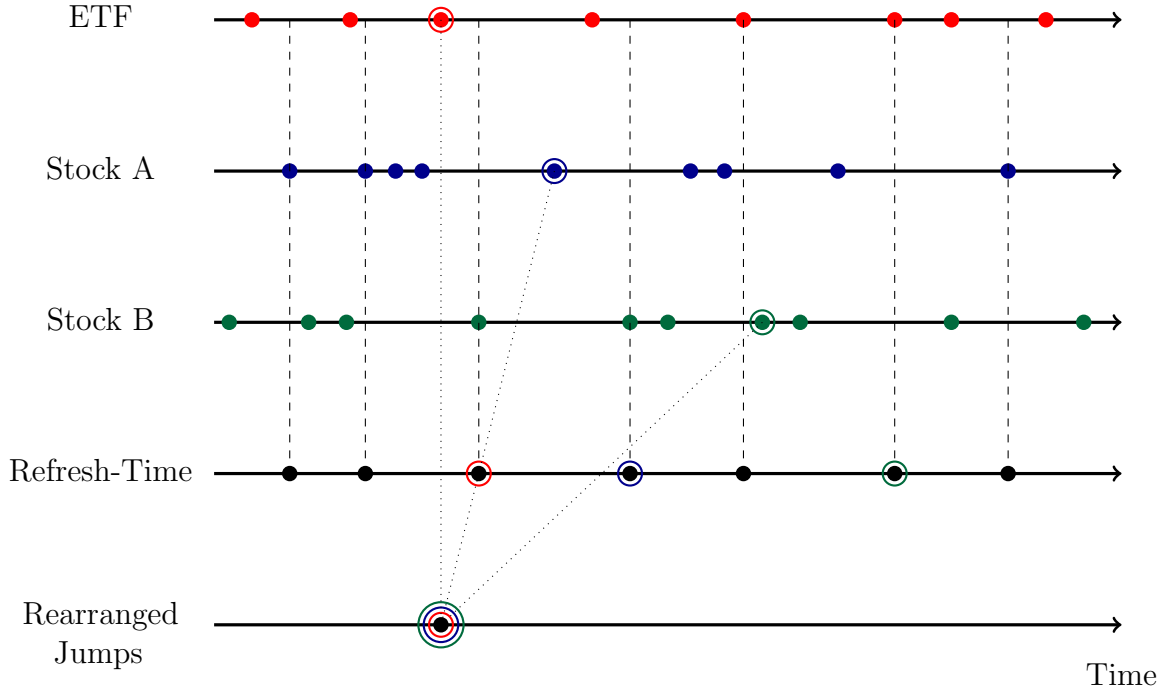
2.1 A DGP for sluggish news reactions

We assume a data generating process for the sluggish prices of the stocks in the index, which features gradual jumps and jump delays.¹ A jump in the underlying equilibrium price may not be immediately reflected in the observed price due to various trading frictions. Such complications are not captured in the standard martingale-plus-noise price model, but they are important in the empirical analysis of multivariate jump processes.

Let $X_t = (X_{1,t}, \dots, X_{p,t})^\top$ denote the logarithmic p -variate, equilibrium (or so-called “efficient”) price of the p stocks in the market index. The price process is defined on a filtered probability space $(\Omega, \mathcal{F}, (\mathcal{F})_{t \geq 0}, \mathbb{P})$ and is adapted to the filtration \mathcal{F}_t that represents information available to market participants at time t , with $t \geq 0$. We assume that X operates in an arbitrage-free, frictionless market, which implies that X is a semimartingale. Econometricians (see Aït-Sahalia and Jacod, 2014) model stock prices X as a jump-diffusion process,

¹Gradual jumps are when the prices exhibit strong linear trends for periods of a few minutes (Barndorff-Nielsen et al., 2009). Jump delays are when jumps of individual assets follow those of the highly liquid market index during market-wide events (Li et al., 2017).

Figure 1: Jump sampling



Note: This figure compares refresh-time sampling to jump sampling in the presence of asynchronous observations and jumps. In each asset's case, the filled dots indicate when the posted prices were updated, and the open dot represents the time at which the price jumps. The vertical dashed lines represent the sampling times generated from the three assets using refresh-time sampling. Jump sampling rearranges mistimed jumps to occur simultaneously with the ETF jump.

which includes a continuous Brownian component and a discontinuous jump component:

$$\begin{aligned}
 X_t &= X_t^c + X_t^d, \text{ with,} \\
 X_t^c &\equiv X_0 + \int_0^t b_s ds + \int_0^t \sigma_s dW_s, \\
 X_t^d &\equiv \sum_{s \leq t} \Delta X_s,
 \end{aligned} \tag{1}$$

in which $t \geq 0$, b is the drift process, σ is the stochastic (co)volatility process, W is a multivariate Brownian motion and $\Delta X_t \equiv X_t - X_{t-}$, with X_{t-} the left limit at time t , denotes the jumps of X at time t . A stock's growth prospects generates a jump in single stock price. Major economic news, such as pre-scheduled announcements, natural disasters or geopolitical conflicts, trigger common (*i.e.* synchronous) jumps in related stock prices (see *e.g.* Li et al., 2017, for some empirical examples).

In practice we do not observe the price process in (1). Instead we observe discretely sampled, noisy transaction prices. Frictions such as tick size, discrete observations, bid-ask spreads, adverse selection, liquidity and inventory control produce market microstructure noise (see *e.g.*, Christensen et al., 2014; Lee and Mykland, 2012; Li and Linton, 2022). Prices may also be sluggish because market participants must trade to reveal private information and reach a consensus about the impact of some piece of news. If trades do not occur at the time a jump in the underlying efficient price occurs, then observed news reactions can be

sluggish because trading is not continuous even if market participants are constantly aware of fundamentals.

We model the observed log price process $Y_t = (Y_{1,t}, \dots, Y_{p,t})^\top$ of the p stocks as contaminated version of (1) observed at discrete intervals:

$$\begin{aligned} Y_{i\Delta_n} &= Y_{i\Delta_n}^c + Y_{i\Delta_n}^d, \text{ with,} \\ Y_{i\Delta_n}^c &\equiv X_{i\Delta_n}^c + u_{i\Delta_n}, \\ Y_{i\Delta_n}^d &\equiv \sum_{h\Delta_n \leq i\Delta_n} \Delta Y_{h\Delta_n}. \end{aligned} \quad (2)$$

There are two kinds of noise: microstructure noise and mistimed jumps. Microstructure noise u contaminates the efficient price process X , but is typically too small to substantially contaminate the discontinuous part X^d . It can neither generate gradual jumps (as in Barndorff-Nielsen et al., 2009) nor jump delays (as in Li et al., 2017). We capture the mistimed or mismeasured jumps in a separate noisy jump component Y^d , which allows a sluggish news reaction, spreading the stock jump across several time intervals.

Figure 2 shows a simulated sample path of this new DGP for 1 stock. The top panel of Figure 2 illustrates that the efficient stock price jumps at 12:45 in reaction to news. In the following 112 seconds, the observed price (in black) catches up with the new equilibrium level (in gray) by gradually matching the jump. The middle and bottom panels respectively decompose the price process into its continuous Brownian component and its jump component. The middle panel compares the efficient, continuous price with the one contaminated by mild market microstructure noise. The bottom panel compares the efficient, sudden jump with the contaminated, gradual jump. Our assumed DGP uses a step function to model how observed prices incorporate news. Appendix A shows how to spread the jump across several time intervals.

The observed price process (2) combines the frictions and the sampling frequency. We sample discretely at time points $i\Delta_n$, with $i = 0, \dots, \lfloor T/\Delta_n \rfloor$, across a time span T , in which $\lfloor \cdot \rfloor$ denotes the floor function. There is less noise on a coarse sampling grid, *i.e.* at a lower sampling frequency Δ_n , but data at such lower frequencies tend to oversmooth actual changes (as in Bollerslev et al., 2008; Lahaye et al., 2011; Li et al., 2019). The finer the sampling grid, the higher the probability that a jump can be recognized as such (Aït-Sahalia, 2004).

2.2 Collecting asynchronous jumps in a jump-event matrix

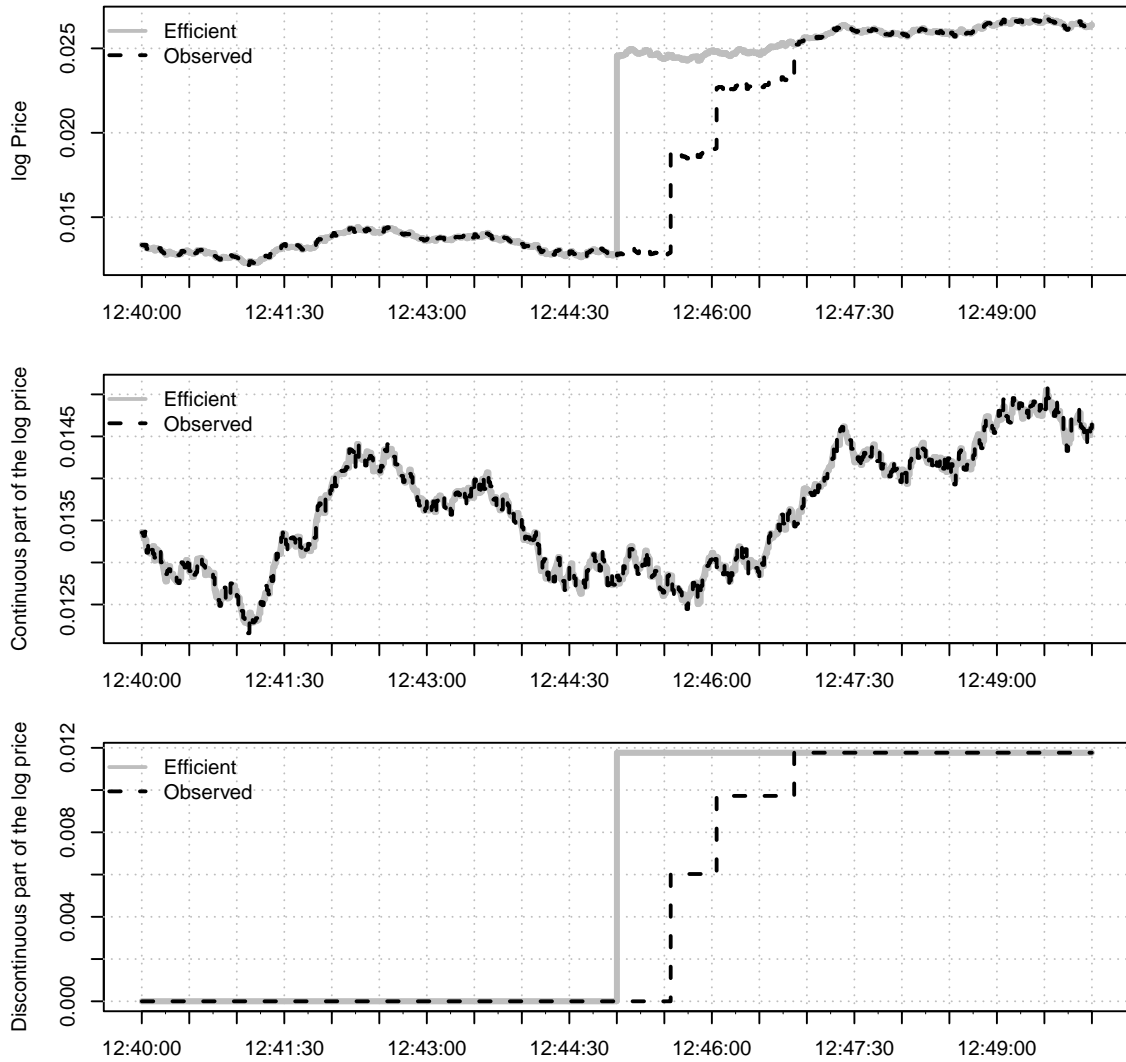
When multiple stocks react sluggishly to new information, their jumps are asynchronous on a fine sampling grid, and these jumps will generally not coincide with the jump in the price of an index tracker. Empirical evidence corroborates this prediction: jumps of less-liquid individual assets typically lag those of the more-liquid market index (Li et al., 2017) and the ETF jumps more often than a synthetically constructed index of stocks (Bollerslev et al., 2008).

2.2.1 The spread measures sluggishness in high-frequency data

Let $w_{k,t}$, with $k = 1, \dots, p$, be the weights allocated to each stock in the market index at each moment in time. The price of the synthetically constructed index portfolio, $S_{i\Delta_n}$, is a linear combination of the observed stock prices in (2), sluggishly incorporating its jump component:

$$S_{i\Delta_n} = \sum_{k=1}^p w_{k,i\Delta_n} Y_{k,i\Delta_n}. \quad (3)$$

Figure 2: The discontinuous component of a stock's price may react sluggishly to news



Note: We plot the decomposition of the efficient (1) and observed (2) log price process for one sample path during a short event window. We simulate second-by-second ($\Delta_n = 1/23,401$) efficient and observed prices for 1 stock across one trading day. The top panel shows the log price. The middle panel shows the continuous part of the log price, and the bottom panel shows the discontinuous part of the log price. The efficient stock price jumps at $i\Delta_n = 11,701$ or 12:45:00. Mild market microstructure noise contaminates the continuous part of the price process, while delays in the jump process contaminate the discontinuous part of the price process.

An ETF log price process, Z_t , tracks an index of the p stocks. We assume that the observed log price Z replicates a portfolio of efficiently priced stocks (1), efficiently incorporating its jump component²:

$$Z_t = \sum_{k=1}^p w_{k,t} X_{k,t}. \quad (4)$$

The deviation or spread in prices is the difference between the observed prices on a

²To simplify our notation, we rely on a weighted average of individual log returns as opposed to simple returns. This difference is considered as minor in empirical applications (Jondeau, Poon, and Rockinger, 2007, pp. 9).

synthetic index of stocks (4) and the prices of an observable ETF trading the index (3):

$$\delta_{i\Delta_n}^p := S_{i\Delta_n} - Z_{i\Delta_n}.$$

Similarly, we can also define the spread in returns as the difference between the observed returns on a synthetic index of stocks $\Delta_i^n S := \sum_{k=1}^p w_{k,i\Delta_n} \Delta_i^n Y_k$ and the returns of an observable ETF trading the index $\Delta_i^n Z := Z_{i\Delta_n} - Z_{(i-1)\Delta_n}$ or, equivalently, the percentage change of the price spread in (5):

$$\delta_{i\Delta_n}^r := \delta_{i\Delta_n}^p - \delta_{(i-1)\Delta_n}^p = \Delta_i^n S - \Delta_i^n Z. \quad (5)$$

We expect the ETF log price Z to nearly equal the synthetic log price S in the absence of sluggish prices. Only microstructure noise would separate the two prices. However, asynchronous jumps cause the price of the synthetic index portfolio to deviate from the presumably efficient price of an ETF tracking the index.³ The sluggish components of jumps are much larger than microstructure noise, so asynchronous impoundment of news drives the spread in prices. Hence, the spread (5) between the ETF price and a synthetically constructed index measures the collective misalignment of noisy stock prices with their efficient levels. The goal is to rearrange jumps in empirical data to minimise the spread and recover the latent efficient price.

To illustrate the workings of our procedures, we consider a stylistic 3-stock universe ($p = 3$) and a corresponding ETF, in which stock prices vary in how quickly they impound news. The stock names A, B and C correspond to the indices $k = 1, 2$ and 3. The ABC ETF price is an equally weighted average of the underlying stocks' efficient prices (4) and the synthetic ABC portfolio is an equally weighted average of the stocks' observed prices (3). The sampling frequency is one minute ($\Delta_n = 1/391$).

Consider the following time series of return vectors of the three stocks and the ABC ETF:

$$\Delta_i^n Y_1 = \begin{bmatrix} \vdots \\ -0.018 \\ -0.031 \\ -0.057 \\ \underline{0.629} \\ \underline{0.651} \\ \vdots \end{bmatrix}, \Delta_i^n Y_2 = \begin{bmatrix} \vdots \\ 0.015 \\ -0.067 \\ -0.029 \\ \underline{1.201} \\ \underline{0.062} \\ \vdots \end{bmatrix}, \Delta_i^n Y_3 = \begin{bmatrix} \vdots \\ -0.120 \\ -0.104 \\ 0.088 \\ 0.017 \\ 0.074 \\ \vdots \end{bmatrix}, \text{ and } \Delta_i^n Z = \begin{bmatrix} \vdots \\ -0.039 \\ -0.071 \\ \underline{0.807} \\ 0.001 \\ 0.073 \\ \vdots \end{bmatrix}, \quad (7)$$

in which the returns are reported in percentages and the jump returns are underlined. Prices asynchronously incorporate news. The first column shows that Stock A jumps gradually and finishes its jump 2 minutes after the ETF in the last column, while the second column shows that stock B's jump is not gradual but 1 minute late and stock C does not jump (third column).

These delays cause the implied (inefficient) returns of the ABC portfolio to deviate from the efficient ABC ETF returns. The sum of the first three columns of the matrix below,

³Within our theoretical model descriptions, the difference between the price of the synthetic index and the ETF price (5) equals microstructure noise component minus the discontinuous component that has not yet been impounded into the observed prices:

$$S_{i\Delta_n} - Z_{i\Delta_n} = \sum_{k=1}^p w_{k,i\Delta_n} u_{k,i\Delta_n} + \sum_{k=1}^p w_{k,i\Delta_n} (Y_{k,i\Delta_n}^d - X_{k,i\Delta_n}^d). \quad (6)$$

This sharp theoretical decomposition is unobservable to the econometrician in empirical data.

which calculates the return spread $\delta_{i\Delta_n}^r$, is the equally weighted, linear combination of the log returns of stocks A, B, and C (the first three columns in (7)), that is, the return on the synthetic ABC portfolio. The fourth column on the left side of the equal sign is the log return of the ABC ETF (the last column in (7)). Their difference, on the right-hand side of equation (8), is the return spread (5), in each of the five periods.

$$\delta_{i\Delta_n}^r = \begin{bmatrix} \vdots \\ \underbrace{1/3.(-0.018 + 0.015 - 0.120)}_{\text{ABC portfolio returns}} - \underbrace{(-0.039)}_{\text{ABC ETF returns}} \\ \underbrace{1/3.(-0.031 - 0.067 - 0.104)}_{\text{ABC portfolio returns}} - \underbrace{(-0.071)}_{\text{ABC ETF returns}} \\ \underbrace{1/3.(-0.057 - 0.029 + 0.088)}_{\text{ABC portfolio returns}} - \underbrace{\frac{0.807}{0.001}}_{\text{ABC ETF returns}} \\ \underbrace{1/3.(\frac{0.629}{0.651} + \frac{1.201}{0.062} + 0.017)}_{\text{ABC portfolio returns}} - \underbrace{0.073}_{\text{ABC ETF returns}} \\ \vdots \end{bmatrix} = \begin{bmatrix} \vdots \\ -0.002 \\ 0.003 \\ -0.807 \\ 0.614 \\ 0.189 \\ \vdots \end{bmatrix}. \quad (8)$$

In the first two periods, the returns to the synthetic index portfolio are almost the same as the returns to the ETF, producing only a small deviation on the right-hand side. In the third period, the ETF price jumps by 0.807%, while the prices of the individual stocks do not move much, leading to a large negative spread. In the fourth and fifth periods, the prices of the portfolio of individual stocks catch up to the ETF jump, leading to large positive spreads.

This stylized example captures the central problem in the analysis of common jumps on a fine sampling grid. If news reached the entire market instantly, was interpreted homogeneously, and trading were continuous, jumps in a group of stocks should presumably occur simultaneously with the ETF index jump and the spreads should be small and random. Sluggish price changes lead to asynchronous jumps, however, and the spread temporarily expands and contracts again.

2.2.2 Decomposition of the spread

To isolate the effect of asynchronous jumps on the spread, we break up the return of synthetic stock index portfolio $\Delta_i^n S$ into its discontinuous and continuous part:

$$\Delta_i^n S := \sum_{k=1}^p w_{k,i\Delta_n} \Delta_i^n Y_k = \sum_{k=1}^p w_{k,i\Delta_n} \Delta_i^n J_k + \sum_{k=1}^p w_{k,i\Delta_n} \Delta_i^n C_k. \quad (9)$$

Jump tests (like Lee and Mykland, 2008) flag some large observed returns as being jumps. We then classify the observed returns as either discontinuous or continuous:

$$\Delta_i^n Y_k = \Delta_i^n J_k + \Delta_i^n C_k \text{ and } \Delta_i^n Z = \Delta_i^n \tilde{J} + \Delta_i^n \tilde{C}, \quad (10)$$

in which $\Delta_i^n Y_k$, for $k = 1, \dots, p$, the i th return of the one-dimensional observed stock log price process, Y_k , is the sum of a discontinuous stock return $\Delta_i^n J_k := \Delta_i^n Y_k \cdot I(\text{Jump}_{i\Delta_n})$ and a continuous stock return $\Delta_i^n C_k := \Delta_i^n Y_k \cdot I(\text{No Jump}_{i\Delta_n})$, in which $I(\cdot)$ is an indicator function. The continuous and sparse jump return vectors are mutually exclusive. A similar classification applies to the ETF return $\Delta_i^n Z$.

The return spread (5) now equals a linear combination of the weighted stock jumps, the

weighted continuous stock returns and the ETF returns:

$$\delta_{i\Delta_n}^r \stackrel{(5)}{:=} \Delta_i^n S - \Delta_i^n Z \stackrel{(9)}{=} \underbrace{\sum_{k=1}^p w_{k,i\Delta_n} \Delta_i^n J_k}_{\text{Weighted discontinuous stock returns}} + \underbrace{\sum_{k=1}^p w_{k,i\Delta_n} \Delta_i^n C_k - \Delta_i^n Z}_{\text{Target}}. \quad (11)$$

We want to synchronize the individual discontinuous jumps (the first element) with the target (the second element) to minimize the return spreads on the event window. If both the stock jumps and the ETF impound news at the same time – the stock jumps offset the target – the spread in returns should be small, containing only microstructure noise.

2.2.3 Constructing the jump-event matrix

To synchronize jumps within an event window, we collect the jump vectors of the individual stocks within a window of observations:

$$[\Delta_i^n J_k]_{i \in \mathcal{W}_n}, \text{ with } k = 1, \dots, p, \quad (12)$$

in which $\Delta_i^n J_k$ is the vector of jump returns for stock k , with $k = 1, \dots, p$, and $\mathcal{W}_n := [I_1\Delta_n, I_2\Delta_n]$ is an event window of size $h \equiv I_2\Delta_n - I_1\Delta_n + 1$. For the empirical application in Section 3, we use an event window from five minutes before to five minutes after the ETF jump, $I_1\Delta_n = (i^* - 5)\Delta_n$ and $I_2\Delta_n = (i^* + 5)\Delta_n$.

To help us rearrange stock jumps, we create an $h \times q$ jump-event matrix J_n , that is an easier-to-handle representation of the decomposition in (11), where h is the number of periods in the window around the ETF jump and $q - 1$ is the number of jumps in individual stocks, where some stocks might jump more than once or not at all:

$$J_n = (\gamma_{il}) := \left[\underbrace{w_{i\Delta_n} \Delta_i^n J}_{\text{Weighted discontinuous stock returns}}, \underbrace{T_{i\Delta_n}}_{\text{Target}} \right]_{i \in \mathcal{W}_n}, \quad (13)$$

in which $i = 1, \dots, h$ and $l = 1, \dots, q$. The first $q - 1$ columns consist of the vectors of weighted stock discontinuous returns $w_{i\Delta_n} \Delta_i^n J := (w_{1,i\Delta_n} \Delta_i^n J_1, \dots, w_{q-1,i\Delta_n} \Delta_i^n J_{q-1})$ sampled within a window of h observations around the ETF jump. The weighted jump vectors $w_{i\Delta_n} \Delta_i^n J$ consist of the p stock jump vectors $\Delta_i^n J_k$, for $k = 1, \dots, p$ in (12), but we reorganize the stock jump vectors. If a stock jumps multiple times, as does stock A, separate jumps appear in different columns. Each jump vector contains one and only one non-zero element. We exclude the jump vectors for which the stock does not jump, as in the case of stock C. The q th column is the target vector, $T_{i\Delta_n} := (\sum_{k=1}^p w_{k,i\Delta_n} \Delta_i^n C_k) - \Delta_i^n Z$, which is the difference between the continuous returns of the synthetic stock index portfolio, $\sum_{k=1}^p w_{k,i\Delta_n} \Delta_i^n C_k$, and the ETF returns $\Delta_i^n Z$. The elements of the target column cannot be moved, while the stock jumps are the moving parts of the jump-event matrix.

Spreads are linear combinations of the stock jumps, the stock's continuous returns and the ETF returns (11). They are the row-sums of the jump-event matrix:

$$J_n^+ := \sum_{m=1}^q (\gamma_{im}) = [\delta_{i\Delta_n}^r]_{i \in \mathcal{W}_n}. \quad (14)$$

The jump-event matrix (13) in our example looks like:

$$J_n = \begin{bmatrix} 0.000 & 0.000 & 0.000 & -0.002 \\ 0.000 & 0.000 & 0.000 & 0.003 \\ 0.000 & 0.000 & 0.000 & -0.807 \\ \underline{0.210} & 0.000 & \underline{0.400} & 0.004 \\ 0.000 & \underline{0.217} & 0.000 & -0.028 \end{bmatrix}, \text{ with row-sums } J_n^+ = \begin{bmatrix} -0.002 \\ 0.003 \\ -0.807 \\ 0.614 \\ 0.189 \end{bmatrix}.$$

Weighted discontinuous stock returns
Target

The first three columns of the jump-event matrix correspond to the individual stock jumps across an event window from two minutes before to two minutes after the ETF jump. Note that the number of columns in the first block corresponds to the number of identified jumps in individual stocks, not the number of individual stocks. The first two columns contain the gradual jumps of Stock A and the third column contains the delayed jump of stock B. The stock jump sizes are generally weighted according to their shares of the index, but this example uses an equally weighted index for simplicity. The fourth column of the jump-event matrix is a target vector that contains the difference between the continuous returns of the stocks and the ETF returns. The return spread is the sum of the row-sums of the weighted discontinuous stock returns and the target column, *i.e.* the row-sums of the jump-event matrix (14). As before (in 2.2.1), there is a negative and a positive spike in the return spread in a small window around the ETF jump in period 3, because stocks A and B do not jump until periods 4 and 5.

2.3 Rearranging the elements within the jump-event matrix

After decomposing the stock returns into jump and non-jump returns, we can rearrange the stock jumps in the jump-event matrix to offset the target column.

2.3.1 Permutations and the return spread after rearrangement

There are different choice options for the rearrangements, making it a combinatorial optimization problem. We seek to rearrange the stock jumps in the jump-event matrix (each individual column in the first block of columns in the jump-event matrix) to offset the elements in the target vector (the last column in the jump-event matrix), which minimizes the variability of return spreads (the row-sums of the jump-event matrix).

A rearrangement (of a particular column in the jump-event matrix) is defined by a permutation π_l of its h elements: $\pi_l : \{1, \dots, h\} \rightarrow \{1, \dots, h\}$, with $l = 1, \dots, q$. The permutation π_l is represented compactly by a vector mapping the original row order into a new row order:

$$\pi_l \equiv (\pi_l(1) \quad \pi_l(2) \quad \dots \quad \pi_l(h)). \quad (15)$$

The vector of q permutations $\pi := (\pi_1, \dots, \pi_q)$ collects the rearrangements of all columns. Note that the q th column, the target, is fixed. We do not swap any elements in the q th column of the jump-event matrix.

Each rearrangement of an observed jump-event matrix (13) yields a new (“rearranged”) jump-event matrix:

$$J_n := \left[\underbrace{w_{i\Delta_n} \Delta_i^n J}_{\text{Weighted discontinuous stock returns}}, \underbrace{T_{i\Delta_n}}_{\text{Target}} \right]_{i \in \mathcal{W}_n} \xrightarrow{\text{Rearrangement}} \left[\underbrace{w_{i\Delta_n} \Delta_i^n J^\pi}_{\text{Rearranged weighted discontinuous stock returns}}, \underbrace{T_{i\Delta_n}}_{\text{Target}} \right]_{i \in \mathcal{W}_n} := J_n^\pi, \quad (16)$$

in which $J_n^\pi = (\gamma_{il}^\pi)$ is the rearranged jump-event matrix, $w_{i\Delta_n} \Delta_i^n J^\pi := (w_{1,i\Delta_n} \Delta_i^n J_1^\pi, \dots, w_{q-1,i\Delta_n} \Delta_i^n J_{q-1}^\pi)$ is the vector of *rearranged* weighted stock jump returns.

The row-sums of the rearranged jump-event matrix J_n^π , *i.e.* the corresponding return spreads, are expressed as a function of the arrangement (and timing) of the stock jumps:

$$J_n^{\pi,+} := \sum_{m=1}^q (\gamma_{im}^\pi)$$

For example, consider the following permutation π_1 (15) of the first column of the jump-event matrix, swapping the 3rd and the 4th observation:

$$\pi_1 = (1 \ 2 \ \underline{4} \ \underline{3} \ 5).$$

This swap rearranges the jump-event matrix, switching the 3rd and 4th rows of the first column:

$$J_n^\pi = \begin{bmatrix} 0.000 & 0.000 & 0.000 & -0.002 \\ 0.000 & 0.000 & 0.000 & 0.003 \\ \underline{0.210} & 0.000 & 0.000 & -0.807 \\ 0.000 & 0.000 & \underline{0.400} & 0.004 \\ 0.000 & \underline{0.217} & 0.000 & -0.028 \end{bmatrix}, \text{ with row-sums } J_n^{\pi,+} = \begin{bmatrix} -0.002 \\ 0.003 \\ -0.597 \\ 0.404 \\ 0.189 \end{bmatrix},$$

Rearranged weighted discontinuous stock returns
Target

which shifts a weighted stock jump of stock A one period back in time (and a zero forward in time). The permutation π_1 also changes the third and fourth row-sum of the jump-event matrix. The variability in the row-sums is slightly smaller after this rearrangement, because the ETF jump also occurs in the third observation.

2.4 The best rearrangement of the jump-event matrix

Under the assumption that the latent prices of the price series of the stocks and the ETF move in lockstep, the best rearrangement moves jumps in time to minimize the variability of the return spreads. This reduction in variability is known as “flattening”.⁴

The optimization problem that minimizes the variance of the return spreads is a combinatorial problem that can be expressed as follows:

$$\min_{\pi} V(J_n^{\pi,+}), \text{ with } J_n^{\pi,+} := \sum_{m=1}^q (\gamma_{im}^\pi), \quad (17)$$

⁴Flattening the row-sums of the jump-event matrix means that the stochastic variables in the separate columns of the jump-event matrix should be completely mixable. Mathematically, a q -dimensional distribution function $F(Q_1, \dots, Q_q)$ on \mathbb{R} is q -completely mixable if there exist q random variables Q_1, \dots, Q_q identically distributed as F such that:

$$\text{Prob}(Q_1 + Q_2 + \dots + Q_q = \text{constant}) = 1.$$

That is, the sums of q random variables drawn from a q -completely mixable distribution should approximate a constant. A completely mixable dependence structure minimizes the variance of the sum of the random variables with given marginal distributions. In a discrete case, like the jump-event matrix which consists of realizations of random variables, we look for a particular ordering in each of the columns, such that the row-sums approximate a constant.

in which the row-sums $J_n^{\pi,+}$ are return spreads expressed as a function of the arrangement of stock jumps, $V(\cdot)$ is a scalar-valued function that measures the variability, *e.g.*, the range, of the vector of row-sums.

The combinatorial optimization problem (17) is rooted in the pioneering work of Puccetti and Rüschendorf (2012) and Embrechts et al. (2013) on rearrangements and the Rearrangement Algorithm; looping over each column of a matrix to order it oppositely to the sum of the other columns (see Appendix B for an example). This algorithm is best known as an actuarial tool to bound portfolio risk, but it also has applications in other disciplines, such as operations research (see *e.g.*, Boudt et al., 2018). The algorithm can propose a best rearrangement of the jump-event matrix (17) but it does not constrain the type of rearrangements that take place. For example, it can move jumps either forward or backward in time to any point in the window.

To constrain the procedure from economically implausible rearrangements, we introduce the Rearrangement Linear Program (RLP) that is well suited to choose arguments which minimize an objective function (2.4.1), subject to linear constraints (2.4.2) and penalties (2.4.3).

2.4.1 Arguments and objective function

There are two types of arguments to the solution function: 1) permutation matrices and 2) an unknown interval within which all the row-sums lie.

Permutation matrices

To rearrange (i.e., permute) a column of the jump-event matrix, we premultiply a column by a permutation matrix. We rely on the column representation of a permutation matrix. Each permutation matrix permutes one column of the jump event matrix, so a solution will include q permutation matrices – 4 columns in the jump-event matrix means there are 4 permutation matrices.

An $h \times h$ permutation matrix permutes the columns of the identity matrix I_h to express a permutation π_l (15):

$$P_{\pi_l} = (p_{ii'}) = \begin{bmatrix} p_{11} & p_{12} & \cdots & p_{1h} \\ p_{21} & p_{22} & \cdots & p_{2h} \\ \vdots & & \ddots & \\ p_{h1} & p_{h2} & \cdots & p_{hh} \end{bmatrix} = \begin{bmatrix} \mathbf{e}_{\pi_l(1)} \\ \mathbf{e}_{\pi_l(2)} \\ \vdots \\ \mathbf{e}_{\pi_l(n)} \end{bmatrix}. \quad (18)$$

For each i , $p_{ii'}$ is 1 if $i' = \pi_l(i)$ and is 0 otherwise. The entries of the i th row are all zero except for a 1 that appears in column $\pi_l(i)$. A standard basis vector, $\mathbf{e}_{i'}$, denotes a row-vector of length h with a 1 on position i' and a 0 on every other position.

We rely on this representation because a permutation matrix (18) can track how far the ones deviate from the diagonal, which permits penalties for movement. For example, we can impose a maximum distance from the diagonal to not let the jumps stray too far in the event window (see Section 2.4.3 for further elaboration).

The permutation in the example of Section 2.3.1, $\pi_1 = (1 \ 2 \ \underline{4} \ \underline{3} \ 5)$, switches the 3rd and 4th rows of the 1st column of a jump-event matrix, and is equivalent to the following

permutation matrix:

$$P_{\pi_1} = \begin{bmatrix} \mathbf{e}_{\pi_1(1)} \\ \mathbf{e}_{\pi_1(2)} \\ \vdots \\ \mathbf{e}_{\pi_1(n)} \end{bmatrix} = \begin{bmatrix} \mathbf{e}_1 \\ \mathbf{e}_2 \\ \mathbf{e}_4 \\ \mathbf{e}_3 \\ \mathbf{e}_5 \end{bmatrix} = \begin{bmatrix} 1 & 0 & 0 & 0 & 0 \\ 0 & 1 & 0 & 0 & 0 \\ 0 & 0 & 0 & 1 & 0 \\ 0 & 0 & 1 & 0 & 0 \\ 0 & 0 & 0 & 0 & 1 \end{bmatrix},$$

in which column i' of the I_5 identity matrix now appears as the column $\pi(i')$ of P_{π_1} . The changes occur in the vertical, i , dimension. Upward moves in the permutation matrix are backward moves in time. Downward moves in the permutation matrix are forward moves in time. The fourth element, which is on position (4,4) in I_5 , shifts one spot backward in time by shifting one step upward in the permutation matrix. The third element, which is on position (3,3) in I_5 , shifts one step forward in time by shifting one step downward in the permutation matrix.

We have a permutation matrix for each of the q columns in the jump-event matrix. We concatenate the permutation matrices in a co-permutation matrix of dimension $h \times (hq)$:

$$\Pi = (p_{l i i'}) = [P_{\pi_1}, P_{\pi_2}, \dots, P_{\pi_q}], \quad (19)$$

with $l = 1, \dots, q$, $i, i' = 1, \dots, h$ and P_{π_l} short notation for the $h \times h$ permutation matrix for the first column of the jump-event matrix.

Premultiplying the (vectorized) jump-event matrix by the co-permutation matrix produces the vector of return spreads:

$$J_n^{\pi,+} = \Pi \times \text{vec}(J_n), \quad (20)$$

or, equivalently:

$$\begin{bmatrix} J_{n,1}^{\pi,+} \\ J_{n,2}^{\pi,+} \\ J_{n,3}^{\pi,+} \\ \vdots \\ J_{n,h}^{\pi,+} \end{bmatrix} = \begin{bmatrix} p_{111} & p_{112} & \dots & p_{11h} & p_{211} & p_{212} & \dots & p_{21h} & \dots & p_{q11} & p_{q12} & \dots & p_{q1h} \\ p_{121} & p_{122} & \dots & p_{12h} & p_{221} & p_{222} & \dots & p_{22h} & \dots & p_{q21} & p_{q22} & \dots & p_{q2h} \\ \vdots & & \ddots & \vdots & \vdots & & \ddots & \vdots & & \vdots & & \ddots & \vdots \\ p_{1h1} & p_{1h2} & \dots & p_{1hh} & p_{2h1} & p_{2h2} & \dots & p_{2hh} & \dots & p_{qh1} & p_{qh2} & \dots & p_{qhh} \end{bmatrix} \times \begin{bmatrix} \gamma_{11} \\ \gamma_{21} \\ \vdots \\ \gamma_{h1} \\ \vdots \end{bmatrix},$$

in which $\text{vec}(J_n)$, the vectorized version of the observed jump-event matrix $J_n = (\gamma_{il})$, with $i = 1, \dots, h$ and $l = 1, \dots, q$, is a stacked column vector of dimension $hq \times 1$. The result of the matrix product in (20) is a $h \times 1$ column vector, including the row-sums of the rearranged jump-event matrix (the left side of the equal sign).

Unknown interval

The RLP chooses a co-permutation matrix that minimizes the range of the row-sum. The range is the difference between the maximum and the minimum order statistic of the row-sums:

$$R = J_{n,(h)}^{\pi,+} - J_{n,(1)}^{\pi,+}. \quad (21)$$

in which the subscript (i) enclosed in parentheses indicates the i th order statistic of the sample: the smallest and a largest row-sum for a particular arrangement.

The positions of the smallest and largest row-sums are unknown upfront. In order to express this objective function within the RLP we slightly deviate from the standard canonical forms of linear programs – the objective function within a linear program is typically an affine function of its arguments.⁵ The co-permutation matrix extracts the row-sum in each row in the matrix product (20), *i.e.*, $J_{n,1}^{\pi,+}, J_{n,2}^{\pi,+}, \dots, J_{n,h}^{\pi,+}$ (without brackets), but there is no possible choice of the co-permutation matrix which could ever produce the maximum or minimum of the row-sums in (21), *i.e.*, $J_{n,(1)}^{\pi,+}$ and $J_{n,(h)}^{\pi,+}$ (with brackets).

We get the appropriate objective function indirectly, by minimizing an unknown interval within which all the row-sums lie:

$$\text{Find } \Pi, L, U \text{ that minimizes } U - L, \quad (22)$$

in which Π is the co-permutation matrix, which defines arrangement of the elements in the rearranged jump-event matrix, U is the upper boundary of an unknown interval and L is the lower boundary of an unknown interval.

The program chooses candidates for both types decision variables – the permutation matrices and the lower and upper boundary of the unknown interval – to minimize the range of that interval (22). The MILP chooses the elements (0,1) for the permutation matrices and continuous values for the lower and upper boundary. The optimization problem (22) is therefore a mixed-integer linear program (MILP).

The optimization in (22) does not minimize the range of the row-sums yet. We must define a permutation within a linear program and connect the lower and upper boundary, L and U with the co-permutation matrix Π by constraining the choices of the decision variables.

2.4.2 Constraints

We constrain the sensible choices of the decision variables using three types of constraints: the ordering constraint, the permutation constraint and a target constraint. The combination of these minimal conditions does lead to appropriate rearrangements which minimize the range.

The ordering constraint

The unconstrained MILP, as it is defined in (22), has a lower and upper boundary of an unknown interval both in the argument and in the objective function. It can choose any continuous value for the lower boundary L (say, a big negative number) and any continuous value for the upper boundary (say, zero) to minimize the difference between these two random numbers. The minimization will push the difference towards a big negative number, because these optimal boundaries are still unconnected to the co-permutation matrix.

We impose inequality constraints on the boundaries:

$$L \leq J_{n,i}^{\pi,+} \leq U, \text{ for } i = 1, \dots, h, \quad (23)$$

in which the row-sums in the middle are the result of the matrix product in (20) for a particular arrangement of jumps. The constraint indirectly defines the smallest possible (the minimum) and largest possible (maximum) row-sum. The left inequality in (23) defines a lower boundary in a set of row-sums (by definition each individual row-sum should greater than or equal to the minimum) and the right inequality defines upper boundary in a set

⁵Linear programs are problems that can be expressed in canonical form as: “Find a vector \mathbf{x} that minimizes $\mathbf{c}^\top \mathbf{x}$, with \mathbf{c} a given vector, subject to some constraints on \mathbf{x} .”

of row-sums (by definition each individual row-sum should be less than or equal to the maximum). The outer boundaries, the lower boundary should be less than or equal to the upper boundary, ensures that the minimum is always smaller than the maximum, as by definition.

Choosing candidate values for the lower and upper boundary (22) still result in values which are unconnected to the row-sums. A big negative number for the lower boundary L will satisfy the constraint (23): L will be smaller than any row-sum. (And a big positive number for the upper boundary will also satisfy the constraint: U will still be larger than any row-sum.) But by minimizing the difference of these decision variables, $U - L$, as defined in (22), the RLP squeezes the outer values in the constraint (23) together, as close as possible. (Note that if we would maximize the range, $U - L$, the lower and outer boundary L and U would move away from each other and from the row-sums.) The optimal solutions for L and U will then be equal to the smallest and largest row-sum:

$$L^* = J_{n,(1)}^{\pi,+} \quad \text{and} \quad U^* = J_{n,(h)}^{\pi,+}, \quad (24)$$

A simple proof by contradiction suffices to confirm this statement. Suppose that L^* is not equal to the smallest row-sum $J_{n,(1)}^{\pi,+}$ or U^* is not equal to the largest row-sum $J_{n,(h)}^{\pi,+}$. In any of those cases, the RLP can still further minimize the objective function $U - L$.

The permutation constraints

To define a proper co-permutation matrix (19), we impose equality constraints on the linear program:

$$\sum_{l=1}^q \sum_{i=1}^h \sum_{i'=1}^h p_{lii'} = hq, \quad (25)$$

$$\sum_{i'=1}^h p_{lii'} = 1, \quad \text{for } i = 1, \dots, h \text{ and } l = 1, \dots, q, \quad (26)$$

$$\sum_{i=1}^h p_{lii'} = 1, \quad \text{for } l = 1, \dots, q \text{ and } i' = 1, \dots, h. \quad (27)$$

The first equation (25) requires that each permutation matrix (18) has h ones to select all (exactly h) elements in each column of the jump-event matrix, so the sum over all permutation matrices in the co-permutation matrix should equal hq . The second equation (26) constrains the rows on each permutation matrix to sum to one. Suppose that the rows of each permutation matrix do not sum to one, then we could have either multiple or zero elements in the rearranged matrix on a particular position. The last equation (27) is a column constraint on the permutation matrix, which guarantees that the same number does not appear twice in a column of the rearranged matrix, even if the rows sum to one.

The target

We also impose an equality constraint on the permutation matrix of the last column, so that the RLP does not rearrange the last column of the jump-event matrix, *i.e.* the target:

$$(\text{diag}(P_{\pi_q}))_i = 1, \quad \text{for } i = 1, \dots, h, \quad (28)$$

The permutation (18) matrix corresponding the q th column of the jump-event matrix P_{π_q} should remain an identity matrix I_n .

2.4.3 Penalties

A linear program is flexible. It allows for the introduction of penalties to prohibit economically implausible rearrangements. For example, we could penalize large moves in time with the aid of a distance matrix. The distance matrix D_n tracks the distance from the diagonal in any permutation matrix P_{π_l} (18) of the same size:

$$D_n = (d_{ii'}) \begin{bmatrix} 0 & 1 & \cdots & h-2 & h-1 \\ 1 & 0 & \cdots & h-3 & h-2 \\ \vdots & \vdots & \ddots & \vdots & \vdots \\ h-2 & h-3 & \cdots & 0 & 1 \\ h-1 & h-2 & \cdots & 1 & 0 \end{bmatrix}. \quad (29)$$

Keeping the elements on the diagonal of a permutation matrix P_{π_l} (18), *i.e.* no moves, results in a zero distance: the diagonal elements in the distance matrix D_n are zero.

The distance matrix also allows us to enforce an economic assumption: the RLP only allows for a rearrangement of jumps backward in time because we assume that stock prices are sluggish and lag the highly liquid and carefully watched ETF, they do not lead it. That is, we only permit stock jumps to be moved to an earlier time (upward moves in the permutation matrix P_{π_l}), not a later time (downward moves in the permutation matrix P_{π_l}). By taking the upper triangular portion of the distance matrix D_n , we can focus on the backward shifts in a permutation matrix P_{π_l} . The upper triangular portion of the distance matrix still tracks the backward distance traveled of *all* elements in a column of the jump-event matrix, because the permutation matrix (18) also tracks the rearrangements of the zeros. To only track the move of a stock jump, we disable the irrelevant columns of the distance matrix: if the price jumps in period $i = i^*$, we set the columns $i' \neq i^*$ of D_n to zero.

To limit the length of jump moves in our rearrangements, we impose an inequality constraint on a distance metric:

$$d(P_{\pi_l}) \leq c, \text{ for } l = 1, \dots, q-1, \quad (30)$$

in which $c \geq 0$ is the maximum permitted length of the backward move and $d(P_{\pi_l})$ is the total distance traveled of a jump within the l th column of the jump-event matrix.⁶ We do not constrain the q th column, because the RLP keeps the target column fixed in constraint (28). It is possible to constrain each stock differently depending on the liquidity of the stock.

Figure 3 shows the range of the spreads, *i.e.*, flatness, and the jump arrival times as a function of the permitted maximum length of the move for each jump in the stylistic jump-event matrix. We allow each jump to move backward in time a maximum of zero, one, two, three, four minutes and solve the RLP for each of these five possible jump-length constraints. The starting range is what we observe: the gradual jump of Stock A (Jump 1 in the 4th period and Jump 2 in the 5th period) and the delayed jump of Stock B (Jump 3 in the 4th

⁶The total number of relevant moves for the l th column in the jump-event matrix is equal to the following matrix product of a vectorized permutation matrix and a vectorized distance matrix:

$$d(P_{\pi_l}) = \text{vecr}(P_{\pi_l}) \times \text{vecr}(D_n)^\top, \text{ for } l = 1, \dots, q. \quad (31)$$

The vectorization, $\text{vecr}(\cdot)$ concatenates the rows of a matrix, as opposed to a standard vectorization which stacks the the columns, producing a $1 \times hq$ row-vector. We transpose the second term after vectorization to get a $hq \times 1$ column-vector. The result of this matrix product is a row-wise multiplication of the elements of the two matrices, which equals the total number of relevant shifts.

period) with a relatively high range of 1.421. The negative slope of the line in the top panel of Figure 3 shows that allowing more backward shifts flattens the return spreads.

The bottom panel shows the arrival periods for the jumps as a function of the permitted length of backward moves. With no backward moves, jumps 1 and 3 arrive in period 4 and jump 2 arrives in period 5. If we permit one backward move for each jump, the RLP moves jumps 1 and 3 to period 3 while if we permit 2 backward moves, the RLP moves all jumps to period 3. The smallest range (0.048) occurs with two backward shifts, aligning all the jumps in the third period in the bottom panel.

Optimally rearranging the jumps, produces the following transformation of the jump-event matrix:

$$J_n = \begin{bmatrix} 0.000 & 0.000 & 0.000 & -0.002 \\ 0.000 & 0.000 & 0.000 & 0.003 \\ 0.000 & 0.000 & 0.000 & -0.807 \\ \underline{0.210} & 0.000 & \underline{0.400} & 0.004 \\ 0.000 & \underline{0.217} & 0.000 & -0.028 \end{bmatrix} \xrightarrow[\text{rearrangement}]{\text{The best}} \begin{bmatrix} 0.000 & 0.000 & 0.000 & -0.002 \\ 0.000 & 0.000 & 0.000 & 0.003 \\ \underline{0.210} & \underline{0.217} & \underline{0.400} & -0.807 \\ 0.000 & 0.000 & 0.000 & 0.004 \\ 0.000 & 0.000 & 0.000 & -0.028 \end{bmatrix} = J_n^\pi.$$

$\underbrace{\hspace{10em}}_{\text{Weighted discontinuous stock returns}}$

 $\underbrace{\hspace{10em}}_{\text{Target}}$

 $\underbrace{\hspace{10em}}_{\text{Rearranged weighted discontinuous stock returns}}$

 $\underbrace{\hspace{10em}}_{\text{Target}}$

Figure 4 shows the implied prices after this optimal arrangement of jump returns. Prices asynchronously incorporate news. That is, the observed (black) prices of stock A and stock B deviate from their efficient (gray) values in the first and second panels. (There are also small deviations in Stock C's observed prices due to a (relatively smaller) contamination of the continuous component.) The fourth panel shows that the delays cause the implied (inefficient) price of the basket of stocks (the ABC portfolio) to deviate from the efficient ABC ETF price. The best rearrangement combines two small jumps of stock A and shifts the jumps of stock B one period backward, aligning the jumps in time. The rearranged price paths (green) are now much closer to the efficient price paths (black) in the 1st, 2nd and 4th panel.

3 Empirics

We apply our methods to investigate the reactions of stock prices in event windows around ETF jumps. We illustrate that synchronizing mistimed stock returns increases the Sharpe ratio of a portfolio allocation strategy.

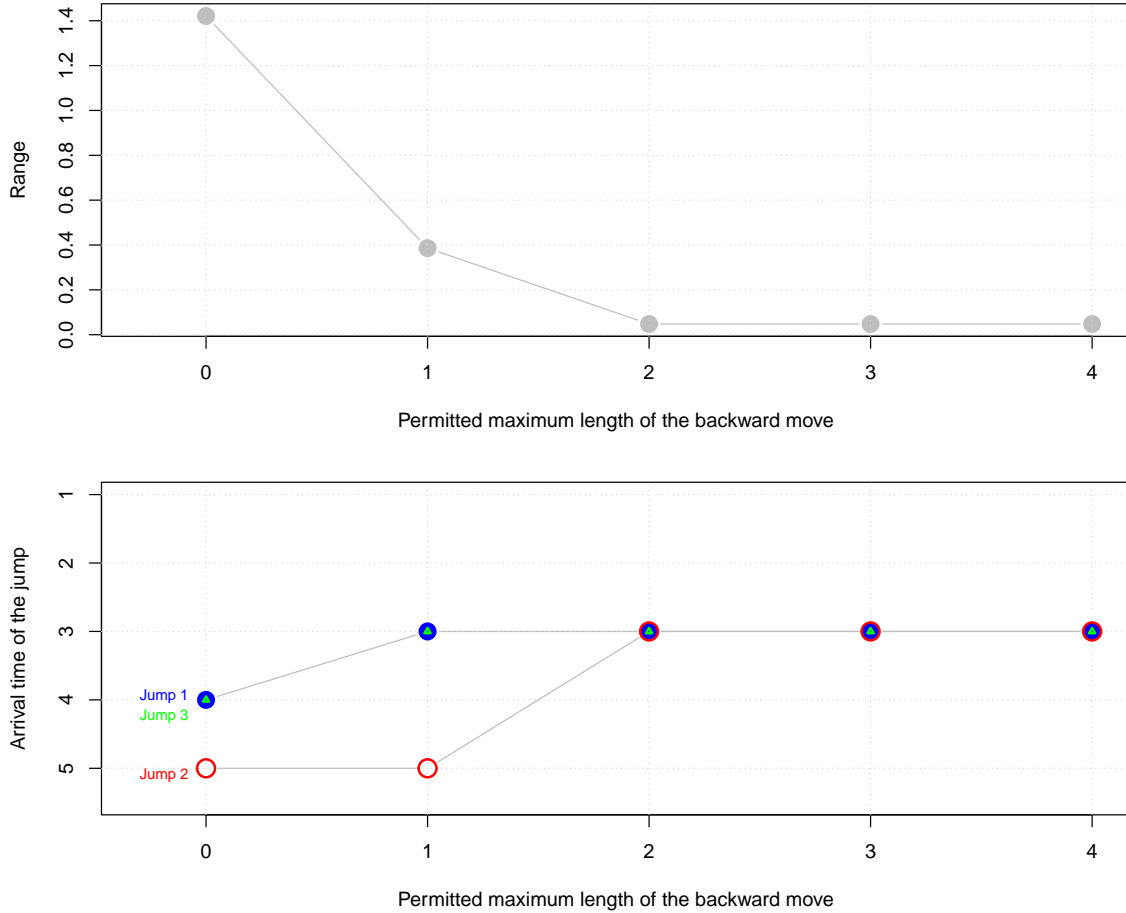
3.1 Data: The Dow and the DIA ETF

The NYSE Trade and Quote (TAQ) database provides equity trade data with millisecond precision timestamps. The basket instrument is the SPDR Dow Jones Industrial Average ETF (DIA). We compare this ETF to the price of a synthetic index of Dow 30 stock prices, as in Bollerslev et al. (2008).⁷

The data cover the period January 3rd, 2007 through April 2nd, 2020, which includes several exceptionally turbulent episodes, such as the global housing and credit crisis, the

⁷The constituency of the Dow 30 index is dynamic. The 43 unique tickers within our sample period are: AA, AAPL, AIG, AXP, BA, BAC, C, CAT, CSCO, CVX, DD, DIS, DOW, DWDP, GE, GM, GS, HD, HON, HPQ, IBM, INTC, JNJ, JPM, KFT, KO, MCD, MMM, MO, MRK, MSFT, NKE, PFE, PG, T, TRV, UNH, UTX, V, VZ, WBA, WMT and XOM.

Figure 3: Trace plot: Range of the spreads and jump arrival times as a function of the permitted maximum length of the move



Note: This figure plots the range of the return spreads (the row-sums of the jump-event matrix) and the implied jump arrival times as a function of the length of permitted backward moves of the jumps in each of the columns. The RLP rearranges the gradual jump of Stock A (Jump 1 in the 4th period and Jump 2 in the 5th period) and the delayed jump of Stock B (Jump 3 in the 4th period). We allow each jump to move backward in time a maximum of zero, one, two, three, four minutes and solve the RLP for each of these five possible constraints.

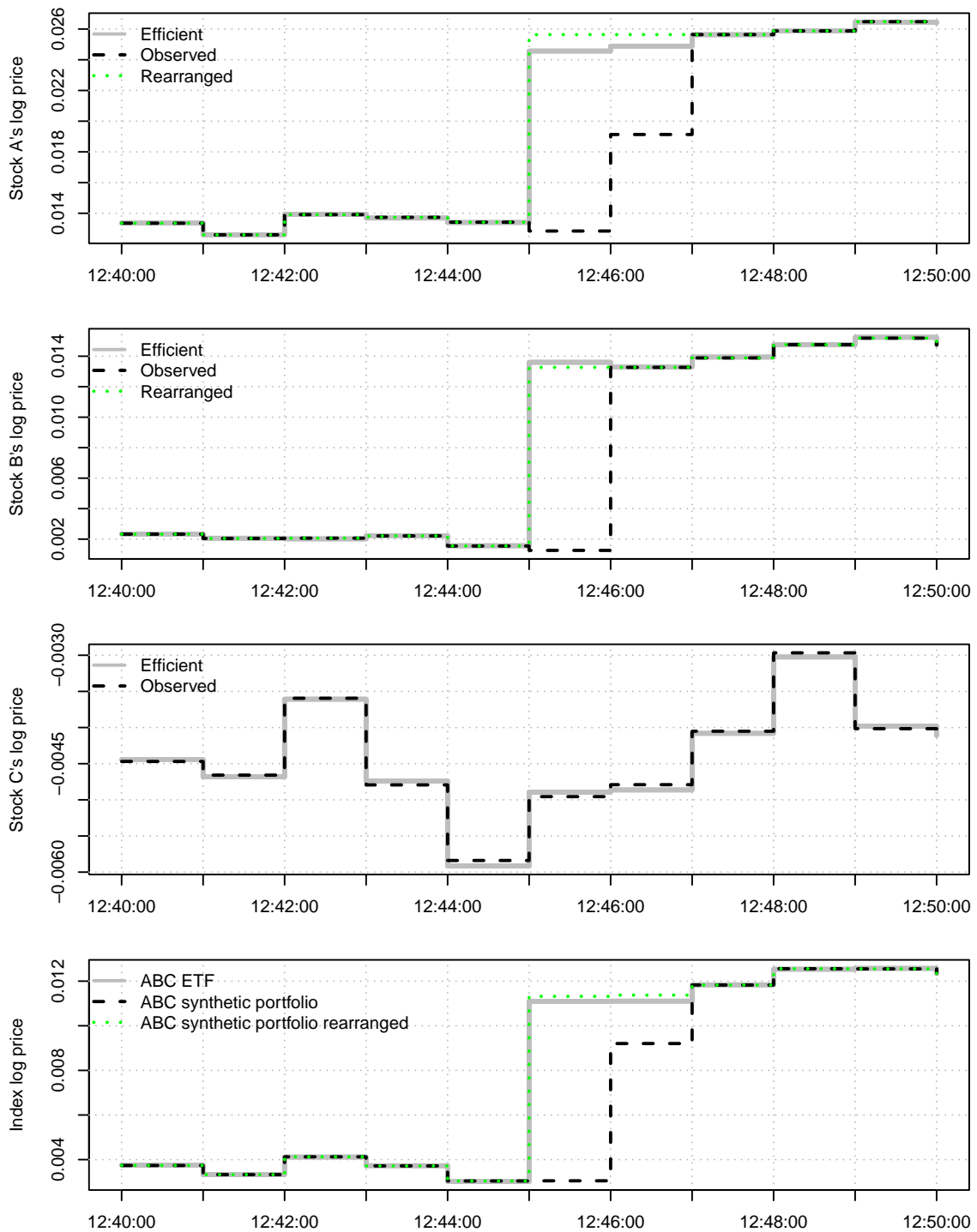
European sovereign debt crisis and the bail-out of Greece, the Russian, Greek, Turkish crisis and the 2020 stock market crash.

We pre-filter the prices as in Barndorff-Nielsen et al. (2009). We also remove banking holidays, half-trading days, any day where there is more than a two-hour gap between consecutive trades and periods of malfunctioning such as the 2010 flash crash.

There are many jumps in the data. We apply Boudt et al. (2011b)'s modified Lee and Mykland (2008)'s univariate jump test that accounts for intraday periodicity, on one-minute returns (at $\alpha = 0.1\%$) to identify jumps. The univariate tests identify 1,710 ETF jumps across 1,163 (jump) days. Some days include gradual or multiple ETF jumps.

There are many asynchronous jumps. We construct 1,529 $[-5,+5]$ -minute jump-event matrices, around ETF jumps, as in equation (13). When there are multiple ETF jumps within the event window, the event window spans from five minutes before the first ETF jump to five minutes after the last jump. We constrain the RLP in three ways. 1) Stocks that already jump with the index, cannot move, because we assume those are efficient. 2)

Figure 4: The best rearrangement approximately recovers the efficient stock jumps



Note: This figure shows the efficient (gray), observed (black) and rearranged (green) log prices of the assets. The top panel shows that Stock A jumps gradually and completes the jump 2 minutes after the ETF in bottom panel, while the second panel shows that stock B's jump is 1 minute late and stock C does not jump at all (third panel). The fourth panel shows that the delays cause the implied (inefficient) price of the basket of stocks (the ABC portfolio) to deviate from the efficient ABC ETF price. The best rearrangement approximately recovers the latent, efficient stock price. That is, by shifting the jumps of Stock A and Stock B to earlier periods (top 2 panels), the LP minimizes the distance between the price of the ETF and the synthetic portfolio (lowest panel).

No stock jumps may be moved earlier than the highly liquid and carefully watched ETF. 3) No stock jumps may be moved if the ETF jumps within the first 10 minutes or the last 10 minutes of the trading day. After imposing these filters, there remain 380 matrices candidate for rearrangement. The RLP rearranges stock jumps in 180 cases (or 11.8% of all jump-event matrices).

3.2 News and asynchronous jumps: An empirical illustration

We investigate sluggish cojumps, *i.e.* jumps that occur later than the index (futures) jumps in the DIA. Consider the following example: on September 18, 2007 the Federal Reserve announced rate cuts, a bold but risky action according to the financial press.⁸

Figure 5 shows the price paths of the DIA ETF and a synthetic Dow 30 index and the spread between the returns of those two assets (5) on the day of the FOMC Statement – September 27, 2008. Lee and Mykland (2008)’s jump test flags a jump at 2:16 pm, one minute after the release of the statement. We mark the ETF jump with a red circle. The ETF price jumps 0.938% at 14:16, U.S. Eastern Time, one minute after the release. As noted before, if news reached the entire market instantly, was interpreted homogeneously, and trading were continuous, jumps in a group of stocks should presumably occur simultaneously with the ETF index jump and spreads should be small and random. The ETF-synthetic index spread temporarily expand, however, following the ETF jump, and then contract again. That is, markets took time to incorporate the Fed’s news into the Dow 30 stock’s prices.

A jump-event matrix (13) characterizes the asset jumps across an event window from five minutes before to five minutes after the index jump. On Sep. 18, 2007, for example, the event window contains 50 stock jumps, including many gradual jumps, from 30 stocks, of which 27 match, *i.e.* occur at the same time as, the ETF jump and 23 lag the ETF jump.

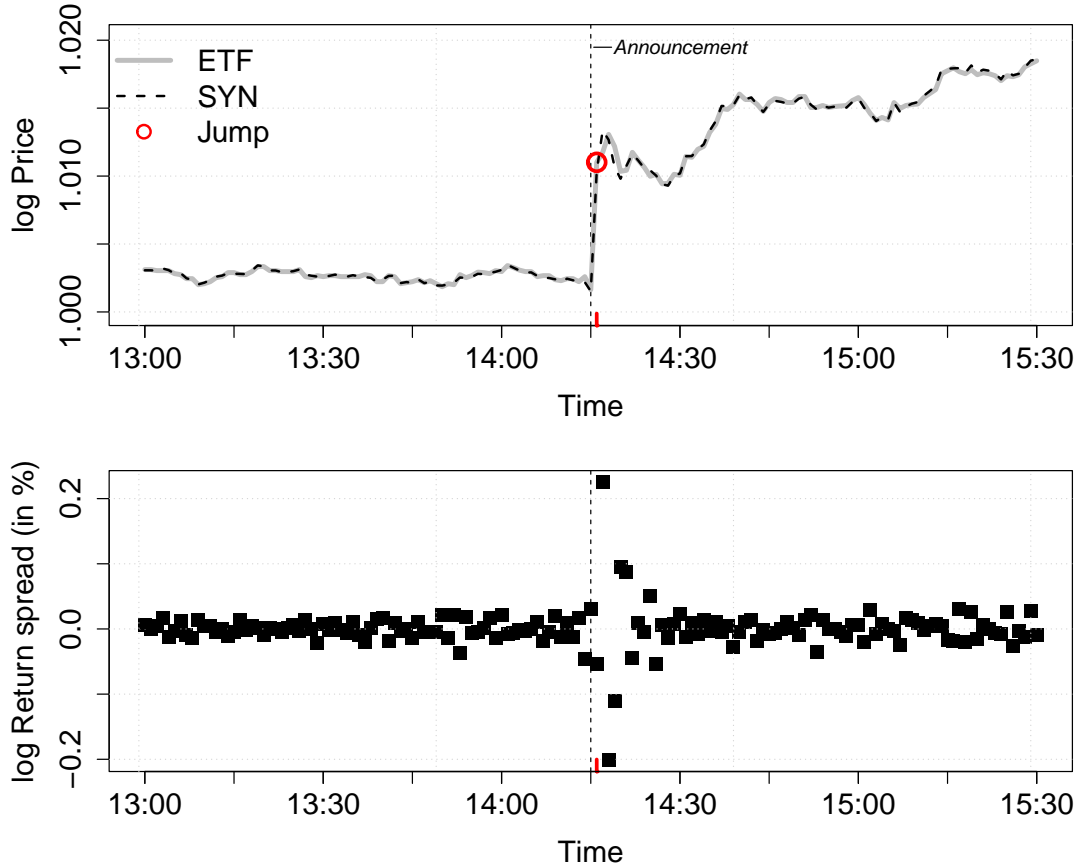
Figure 6 shows the best rearrangement of the stock jumps for this event. By “best rearrangement,” we mean the jump arrangement that minimizes the range of the spreads. The figure shows the range of the return spreads (left scale, gray) and the number of matched stocks (right scale, black) as a function of the permitted length of the move in time for each individual jump, as in equation (30). The range declines as we permit larger moves in time and it is the criterion that determines the chosen number of backward moves for jumps. Permitting each jump to move one minute backward minimizes the range (orange line); the range drops from 0.427% to 0.227%. Permitting a maximum backward repositioning length of 4 periods or 4 minutes (green line) has the same minimal range for a larger number of matching stocks. This rearrangement matches 19 out of 23 scattered stock jumps with the ETF jump, approximately recovering the common jump in the stocks.

Recovering the common jump is likely to improve estimates of the daily realized covariance matrix. The realized covariance matrix is defined as (Barndorff-Nielsen and Shephard, 2004):

$$C_d = \sum_{i=1}^{\lfloor T/\Delta_n \rfloor} (\Delta_i^n Y)(\Delta_i^n Y)^\top \quad (32)$$

⁸The Press release and the related FOMC Meeting Statement. See also the coverage in The Economist and the Financial Times: Bernanke’s bounty, Instant reaction: Response to the Fed, The Short View: Fed decision — it’s all about game theory, Overview: US equities and oil surge after rate cuts, Cheering greets Fed announcement, Fed must weigh inflation against recession, Bold Fed goes for half-point cut, Bank acts boldly to avert recession risk, Fed cut: Pundits speak, Fed slashes rates, and Feeling ecstatic? Mind the e-Ben-der

Figure 5: When the FOMC statement is released on Sep. 18, 2007, the synthetic index-ETF spread expands and contracts again

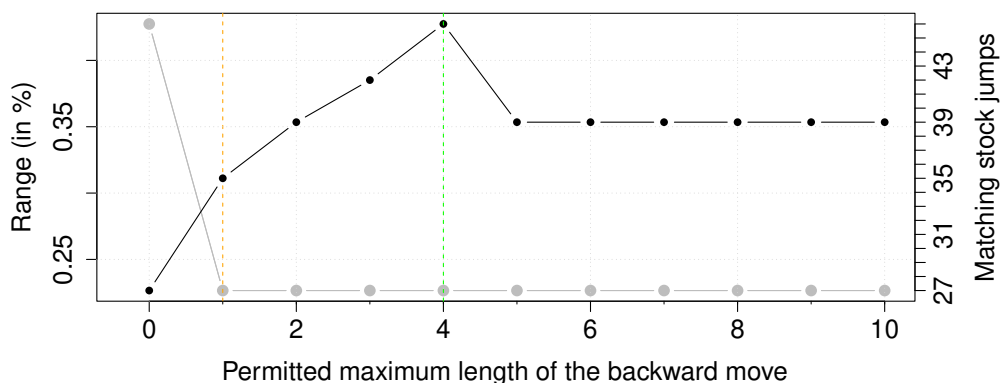


Note: We plot the one-minute log prices of the DIA ETF (in gray) and a synthetically constructed Dow 30 index (in black), alongside the log return spreads, on the day of the FOMC Statement of September 18, 2007. The statement gets issued at 2:15 pm and is marked in the top plot by a dashed line. The subsequent ETF jump at 2:16 pm is marked with a red circle and a red vertical tick on the time axis.

in which, $Y_{i\Delta_n} = (Y_{1,\Delta_n}, \dots, Y_{p,\Delta_n})^\top$ is the observed log price process (2) of the p stocks sampled on a regular time grid $\{i\Delta_n : 0 \leq i \leq \lfloor T/\Delta_n \rfloor\}$ over one day $T = 1$, the i th return of $Y_{i\Delta_n}$ is $\Delta_i^n Y = Y_{i\Delta_n} - Y_{(i-1)\Delta_n}$. The standard realized covariance matrix (32) plugs in raw returns. Other estimators, like the multivariate realized kernel in Barndorff-Nielsen et al. (2011) or a Cholesky factorization in Boudt et al. (2017), protect against mild market microstructure noise and the Epps (1979) effect, that is, the downward bias in covariance estimates due to asynchronous trading. Using rearranged returns in (32) also protects against asynchronous jumps and the underestimation of jump dependence.

Figure 7 allows us to visually compare covariance estimates made with raw *vs.* rearranged returns. It suggests that optimally changing the time labels of one of two observations (out of the 390 one-minute returns required to estimate the realized covariance) changes the estimated covariance structure between the stocks and the ETF returns on the day of the FOMC statement. For example, the fact that the statistics in the left panel generally lay above the 45-degree line shows that rearranging the jumps of HPQ, which jumps gradually, increases its variance and most covariance with other stocks. The right panel shows that rearranging the jumps of PFE, which jumps with an overreaction, reduces its own variance

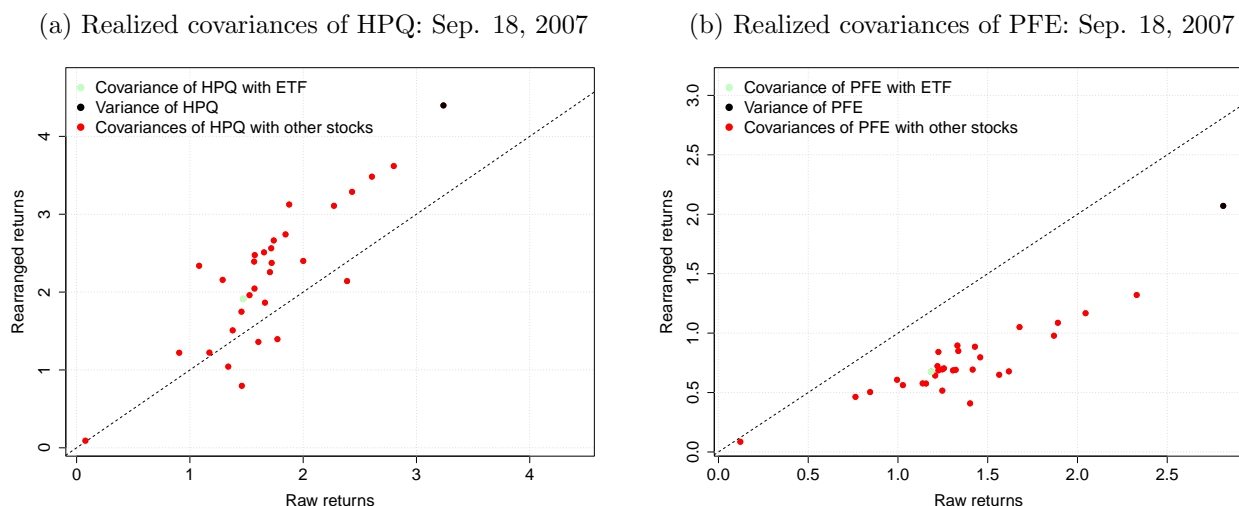
Figure 6: Range of the spreads and matching stocks as a function of the permitted maximum length of the move



Note: This figure plots the range of the return spreads (left scale, gray) and the number of matching stocks (right scale, black) as a function of the number of the permitted length of the move during the Sep. 18, 2007 FOMC statement. The RLP rearranges scattered jumps of the Dow 30 stocks. We allow each jump to move at most 10 minutes backward in time and solve the RLP for each of these possible constraints. We mark the rearrangement with minimal range with an orange line and the rearrangement with the maximum number of matching stock jumps (for the same minimal range) with a green line.

and all the covariances with PFE returns.

Figure 7: The realized covariance is different in the rearranged returns on the day of the FOMC statement



Note: This figure shows two scatter plots consisting of the elements in the realized covariance matrix for two stocks (HPQ and PFE), relative to DIA and the other Dow 30 stocks, on the day of the FOMC statement. The x-axis shows the realized covariances with raw returns and the y-axis the realized covariances with rearranged returns.

A practical question is whether one should use either raw returns or rearranged returns. Our recommendation is to always use the rearranged returns. These synchronized returns are more precise in a high-frequency analysis of market reactions around jumps.

3.3 Minimum-variance portfolios

We show the usefulness of using rearranged returns, compared to using raw returns, in the context of portfolio allocation, which shows that high-frequency rearranged jump returns affect the performance of low-frequency decisions, like building a daily-rebalanced minimum-variance portfolio.

Stock returns determine the weights that minimize the portfolio variance. The optimal weights for a particular day minimize the portfolio variance, subject to the constraints that they deliver a given expected return and that they sum to one (Markowitz, 1952):

$$\underset{w_d}{\text{Minimize}} \sigma_{p,d}^2 = w_d' C_d w_d, \text{ s.t. } w_d' \mu = \mu_{p,d} \text{ and } w_d' 1, \quad (33)$$

in which $\sigma_{p,d}^2$ is the daily variance of the portfolio return, $w_d = (w_{1,d}, \dots, w_{p,d})^\top$ is the daily p -dimensional weight vector, C_d is the daily realized covariance matrix and $\mu_{p,d}$ is the target portfolio return. We make a grid of 100 target returns that range from the lowest average stock return to the highest one. To test our synchronization procedure, compare a simulated portfolio's performance using raw vs. rearranged returns to compute the realized covariance matrix.

We optimize weights (33) on rearrangement days, *i.e.* the 184 ETF jump days for which we rearrange jumps and rebalance the portfolio the next day. We keep those weights until the next rearrangement day. In those cases when the Dow constituency changes in between rearrangement days, we reset to an equally weighted portfolio until the next rearrangement day.

Table 1 reports the portfolios' closing value, standard deviation and modified Sharpe ratio at the 5% level and the p -value of their difference (Ardia and Boudt, 2015) for the full sample and for each year. For 12 of 14 years and over the whole sample, the rearranged-return portfolio statistics are superior to the raw-returns portfolio statistics in terms of the modified Sharpe ratio. Over the full sample, the modified Sharpe ratios are significantly different and the rearranged-return portfolio delivers an additional 5% performance.

4 Concluding remarks

Stock prices often react sluggishly to news, producing gradual jumps and jump delays. The spread between the ETF price and the price of a synthetically constructed index measures the collective misalignment of noisy stock prices with their respective equilibrium levels. We introduce tools to synchronize the scattered jumps in a jump-event matrix and better approximate the efficient common jump. The rearrangement is currently very practical for problems with up to 30 stocks. We are working on a block rearrangement to allow for larger dimensions and, for example, synchronize stock jumps in the S&P500 index.

Estimating realized covariance matrices with these synchronized stock returns, as opposed to using raw returns, improves out-of-sample portfolio performance. Recovering the common jump on a fine sampling grid is likely to improve other asset allocation and risk management decisions, like estimating the jump size distribution (see *e.g.*, Boudt et al., 2011a), estimating jump dependence (see *e.g.*, Li, Todorov, Tauchen, and Chen, 2017; Li, Todorov, and Tauchen, 2017; Li, Todorov, Tauchen, and Lin, 2019) or forecasting realized measures (see *e.g.*, Andersen et al., 2007; Bollerslev et al. 2020; Bollerslev et al., 2022). A thorough analysis must, however, await future work.

Table 1: Performance of minimum-variance portfolios

	Days	#CJ	#CJ-R	Closing value		SD		mSharpe		<i>p</i> -value
				Raw	Rearr.	Raw	Rearr.	Raw	Rearr.	
Full period	3,264	1,163	184	1.8500	1.9000	0.7410	0.7410	0.0159	0.0178	0.0879
Year-by-year										
2007	246	57	13	1.0191	1.0294	0.5592	0.5652	0.0357	0.0430	0.2520
2008	247	55	6	0.9900	0.9880	1.5156	1.5043	0.0377	0.0378	0.9970
2009	243	68	11	1.0607	1.0684	0.9220	0.9254	-0.0127	-0.0110	0.2700
2010	247	65	5	1.0213	1.0384	0.6292	0.6324	-0.0373	-0.0295	0.0919
2011	247	72	6	1.1505	1.1537	0.6268	0.6219	0.0628	0.0644	0.5500
2012	245	107	8	0.9439	0.9493	0.5045	0.5056	-0.0634	-0.0609	0.2950
2013	245	90	13	1.1049	1.0965	0.4865	0.4864	-0.0034	-0.0101	0.1130
2014	247	78	15	1.2607	1.2510	0.4790	0.4730	0.2310	0.2260	0.5180
2015	247	72	9	1.0135	1.0211	0.6918	0.6843	-0.0061	-0.0006	0.4530
2016	249	101	14	1.1480	1.1482	0.5113	0.5109	0.0118	0.0119	0.9860
2017	247	133	23	1.1220	1.1234	0.2977	0.2986	0.0692	0.0709	0.6880
2018	245	93	14	0.9231	0.9310	0.8102	0.8278	0.0254	0.0302	0.4400
2019	246	140	42	1.0817	1.0921	0.5076	0.5123	-0.0028	0.0040	0.2380
2020	63	32	5	1.0135	1.0140	1.5388	1.5407	-0.0021	-0.0017	0.8820

Note: This table reports the performance of the daily returns of a minimum-variance portfolio optimization with raw *vs.* rearranged returns. From left to right, the columns report the number of days (Days), the number of ETF jumps or cojump days (#CJ) and the number of cojump days on which the rearrangement moves stock jumps (#CJ-R). “Closing value” is the end-of-sample portfolio value if the initial value was \$1 using cumulative daily returns. “SD” and “mSharpe” are the standard deviations and modified Sharpe ratios and the *p*-value of their difference (Ardia and Boudt, 2015) of the portfolio over the sample. Gray cells denote the higher of each performance statistic two Sharpe ratios. Dark gray cells denote the significant differences of the two Sharpe ratios at a significance level of 10%. To calculate the modified Sharpe ratio, we use excess returns *vs.* the DIA ETF. To perform the inference of the difference in Sharpe ratios, we rely on the studentized circular bootstrap approach, with 1000 bootstrap replications and a block length of 5 in the circular bootstrap.

References

- Aït-Sahalia, Y. (2004). Disentangling diffusion from jumps. *Journal of Financial Economics* 74(3), 487–528.
- Aït-Sahalia, Y. and J. Jacod (2014). *High-frequency financial econometrics*. Princeton University Press.
- Andersen, T. G., T. Bollerslev, and F. X. Diebold (2007). Roughing it up: Including jump components in the measurement, modeling, and forecasting of return volatility. *Review of Economics and Statistics* 89(4), 701–720.
- Ardia, D. and K. Boudt (2015). Testing equality of modified sharpe ratios. *Finance Research Letters* 13, 97–104.
- Bandi, F. M., D. Pirino, and R. Renò (2017). Excess idle time. *Econometrica* 85(6), 1793–1846.
- Barndorff-Nielsen, O. E., P. R. Hansen, A. Lunde, and N. Shephard (2009). Realized kernels in practice: Trades and quotes. *Econometrics Journal* 12(3), C1–C32.

- Barndorff-Nielsen, O. E., P. R. Hansen, A. Lunde, and N. Shephard (2011). Multivariate realised kernels: consistent positive semi-definite estimators of the covariation of equity prices with noise and non-synchronous trading. *Journal of Econometrics* 162(2), 149–169.
- Barndorff-Nielsen, O. E. and N. Shephard (2004). Econometric analysis of realized covariation: High frequency based covariance, regression, and correlation in financial economics. *Econometrica* 72(3), 885–925.
- Bernard, C., O. Bondarenko, and S. Vanduffel (2018). Rearrangement algorithm and maximum entropy. *Annals of Operations Research* 261(1), 107–134.
- Bernard, C., L. Rüschendorf, and S. Vanduffel (2017). Value-at-risk bounds with variance constraints. *Journal of Risk and Insurance* 84(3), 923–959.
- Bollerslev, T., T. H. Law, and G. Tauchen (2008). Risk, jumps, and diversification. *Journal of Econometrics* 144(1), 234–256.
- Bollerslev, T., J. Li, A. J. Patton, and R. Quaedvlieg (2020). Realized semicovariances. *Econometrica* 88(4), 1515–1551.
- Bollerslev, T., A. J. Patton, and R. Quaedvlieg (2022). Realized semibetas: Disentangling “good” and “bad” downside risks. *Journal of Financial Economics* 144(1), 227–246.
- Boudt, K., C. Croux, and S. Laurent (2011a). Outlyingness weighted covariation. *Journal of Financial Econometrics* 9(4), 657–684.
- Boudt, K., C. Croux, and S. Laurent (2011b). Robust estimation of intraweek periodicity in volatility and jump detection. *Journal of Empirical Finance* 18(2), 353–367.
- Boudt, K., E. Jakobsons, and S. Vanduffel (2018). Block rearranging elements within matrix columns to minimize the variability of the row sums. *4OR* 16(1), 31–50.
- Boudt, K., S. Laurent, A. Lunde, R. Quaedvlieg, and O. Sauri (2017). Positive semidefinite integrated covariance estimation, factorizations and asynchronicity. *Journal of Econometrics* 196(2), 347–367.
- Christensen, K., R. C. Oomen, and M. Podolskij (2014). Fact or friction: Jumps at ultra high frequency. *Journal of Financial Economics* 114(3), 576–599.
- Embrechts, P., G. Puccetti, and L. Rüschendorf (2013). Model uncertainty and VaR aggregation. *Journal of Banking & Finance* 37(8), 2750–2764.
- Epps, T. W. (1979). Comovements in stock prices in the very short run. *Journal of the American Statistical Association* 74(366a), 291–298.
- Jondeau, E., S.-H. Poon, and M. Rockinger (2007). *Financial modeling under non-Gaussian distributions*. Springer Science & Business Media.
- Lahaye, J., S. Laurent, and C. J. Neely (2011). Jumps, cojumps and macro announcements. *Journal of Applied Econometrics* 26(6), 893–921.
- Lee, S. S. and P. A. Mykland (2008). Jumps in financial markets: A new nonparametric test and jump dynamics. *Review of Financial Studies* 21(6), 2535–2563.

- Lee, S. S. and P. A. Mykland (2012). Jumps in equilibrium prices and market microstructure noise. *Journal of Econometrics* 168(2), 396–406.
- Li, J., V. Todorov, and G. Tauchen (2017). Jump regressions. *Econometrica* 85(1), 173–195.
- Li, J., V. Todorov, G. Tauchen, and R. Chen (2017). Mixed-scale jump regressions with bootstrap inference. *Journal of Econometrics* 201(2), 417–432.
- Li, J., V. Todorov, G. Tauchen, and H. Lin (2019). Rank tests at jump events. *Journal of Business & Economic Statistics* 37(2), 312–321.
- Li, Z. M. and O. Linton (2022). A remedy for microstructure noise. *Econometrica* 90(1), 367–389.
- Markowitz, H. (1952). Portfolio selection*. *Journal of Finance* 7(1), 77–91.
- Puccetti, G. and L. Rüschendorf (2012). Computation of sharp bounds on the distribution of a function of dependent risks. *Journal of Computational and Applied Mathematics* 236(7), 1833–1840.

A Simulating sluggish news reactions

We show how to generate a sample path from the new DGP, in which the discontinuous component is spread across several time intervals. We first simulate second-by-second ($\Delta_n = 1/23,401$) efficient log prices (1) for 1 stock ($p = 1$), $X_{i\Delta_n}$, across one trading day ($T = 1$) from a jump-diffusion process.

A.1 The continuous component

The continuous component, $X_{i\Delta_n}^c$, has a zero drift and constant variance $\sigma_t^2 = 0.039$, corresponding to an annualized return volatility of 20%. We add *i.i.d.* microstructure noise u , with $E[u] = 0$ and $E[u^2] = \omega^2$, in which we select ω^2 by fixing the noise ratio to $\gamma = (n\omega^2 / \int_0^1 \sigma_s^2 ds)^{1/2} = 0.5$, to contaminate the continuous part of the efficient price (as in Christensen et al., 2014).

A.2 The discontinuous component

Econometricians typically assume a compound Poisson for the efficient jump process:

$$X_{i\Delta_n}^d \equiv \sum_{j=1}^{N^J} I_{\{U_j \cdot T \leq i\Delta_n\}} \Delta X_j, \quad (34)$$

in which $I(\cdot)$ is an indicator function, N^J is the number of jumps that occur during a day, U_j are the random arrival times of the jumps and the sequence of normally distributed random variables, $\Delta X_1, \dots, \Delta X_{N^J}$, are normally distributed jump sizes.

The news that generates the jump in the efficient price is not immediately impounded in the stock’s observed price. To simulate such a sluggish news reaction, we draw a contaminated

jump process, $Y_{i\Delta_n}^d$, which includes a step function that spreads each individual efficient jump size, ΔX_j , within the compound Poisson process (34), across several time intervals:

$$Y_{i\Delta_n}^d \equiv \sum_{j=1}^{N^J} I_{\{U_j \cdot T \leq i\Delta_n\}} \underbrace{\sum_{d=0}^{N_j^D} I_{\{W_{j,d} \cdot T \leq i\Delta_n\}} \Delta L_{j,d}}_{\text{Progress to efficiency}} \Delta X_j. \quad (35)$$

in which N_j^D governs the total number of steps within each jump's delay process, $W_{j,0}, \dots, W_{j,N_j^D}$ are the step arrival times and $\Delta L_{j,0}, \dots, \Delta L_{j,N_j^D}$ are increments in the step sizes, which add chunks of the efficient jump size, ΔX_j , to the observed jump process, Y^d . The step function captures the progress to efficiency; it rises from 0 to 1 as information about the efficient jump is fully incorporated in the stock's observed price.

A.2.1 Step widths

Suppose an efficient price jumps at the random arrival time, U_j , with a jump size, ΔX_j . To simulate the step function within for this particular jump, we first draw the number of steps, N_j^D , from a binomial distribution:

$$N_j^D \sim \text{Bin}(\text{Number of trials} = 5, \text{Success probability} = 0.4), \text{ for } j \text{ fixed.}$$

Each of the steps has a random width. An exponential distribution governs the waiting times between the steps:

$$w_{j,d} \sim [\text{Exp}[\text{Rate} = 1/(15 N_j^D)]], \text{ for } j \text{ fixed and } d = 1, \dots, N_j^D,$$

in which $[\cdot]$ is the ceiling operator. The step arrival times, $W_{j,d}$, in the indicator function of the compound information process are the cumulative sums of the waiting times starting at the arrival time of the efficient jump U_j :

$$\begin{aligned} W_{j,0} \cdot T &\equiv U_j \cdot T \quad , \\ W_{j,1} \cdot T &\equiv U_j \cdot T + w_{j,1}, \\ W_{j,2} \cdot T &\equiv U_j \cdot T + w_{j,1} + w_{j,2}, \\ &\vdots \\ W_{j,N_j^D} \cdot T &\equiv U_j \cdot T + D_j. \end{aligned}$$

The starting point of the step function, $W_{j,0}$, is the arrival time of the efficient jump. The end point, W_{j,N_j^D} , or the moment when the information has been fully impounded, is the starting point plus the sum of the waiting times. The total delay with which the efficient stock jump is impounded in the observed price is the sum of the waiting times: $D_j = \sum_{d=1}^{N_j^D} w_{j,d}$. If it takes more steps to incorporate the efficient jump, the total delay will be longer.

A.2.2 Step sizes

The steps also have random sizes that correspond to accumulated information impounded in the observed price. To extract the sizes, $L_{j,d}$, of each step d , with $d = 0, \dots, N_j^D$, we sample realizations from a Brownian bridge according to the step arrival times, $W_{j,0}, \dots, W_{j,N_j^D}$.

The Brownian bridge

The Brownian bridge models the latent news impoundment process. When news is released, the market processes and accumulates information, including under- and overreactions. Eventually, the price fully and correctly impounds the information.

The Brownian bridge, $\Lambda_{j,t}$, is a continuous-time, stochastic process defined as:

$$\Lambda_{j,t} = B_{j,t} - \frac{t}{U_j \cdot T + D_j} (1 - B_{j,U_j \cdot T + D_j}), \quad t \in [U_j \cdot T, U_j \cdot T + D_j]$$

in which $B_{j,t}$ is a standard, univariate Wiener process, with $B_{j,0} = 0$. A standard Wiener process is tied down to the origin, but the other points are not restricted. The Brownian bridge is pinned at both ends interval, at $t = U_j \cdot T$ and $t = U_j \cdot T + D_j$. Just as pylons support a literal bridge, the pylons in the Brownian bridge make sure that the process evolves from the first pylon $\Lambda_{j,U_j \cdot T} = 0$ to the second pylon $\Lambda_{j,U_j \cdot T + D_j} = 1$.

Sampling step sizes from the Brownian bridge

The variable governed by the Brownian bridge gradually moves from 0 to 1 – non-monotonically – but we observe its values at discrete intervals, because investors impound chunks of new information in the observed price at each interval. We sample the step sizes from the Brownian bridge process $\Lambda_{j,t}$ at discrete points, $W_{j,0}, W_{j,1}, \dots, W_{j,N_j^D}$.

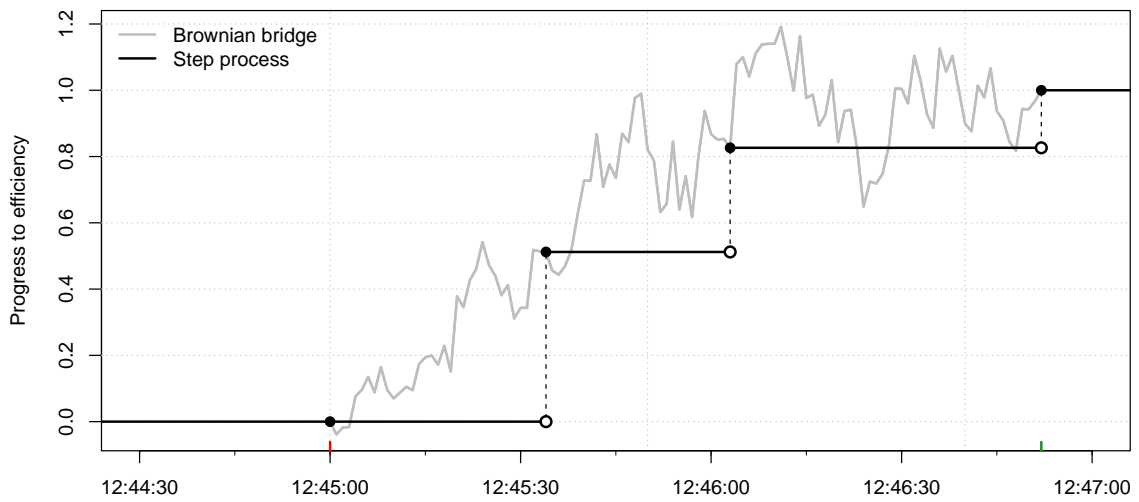
The Brownian bridge and the waiting times exist in continuously observed prices and are functions of the data generating features that delay jumps. They have nothing to do with the data frequency used by the econometrician.

A.2.3 Example of a step function

Figure 8 plots an example of such a step function for one delayed jump. The efficient stock price jumps at $i\Delta_n = 11,701$ or 12:45:00. The waiting times between each of three steps are equal to $w_{1,1} = 34, w_{1,2} = 29, w_{1,3} = 49$ seconds. In the following $D_j = 112$ seconds, the Brownian bridge (in black) process evolves from 0 to 1. If $\Lambda_{j,i\Delta_n} < 1$, the observed price jump underreacts and does not (completely) incorporate the new information. If $\Lambda_{j,i\Delta_n} > 1$, the observed price overreacts to the jump. At the end of the interval, when $\Lambda_{j,i\Delta_n} = 1$, the observed stock jump equals the efficient stock jump.

We do not observe this learning process in continuous time. Rather, we sample the step sizes at the waiting times, leading to the step function (in blue). The waiting times relate to the step widths and are equal to $W_{1,0} \cdot T = 11,701 + 0, W_{1,1} \cdot T = 11,701 + 34, W_{1,2} \cdot T = 11,701 + 63$ and $W_{1,3} \cdot T = 11,701 + 112$. The sampled sizes are equal to 0.000, 0.512, 0.826, and 1.000 and the increments are equal to $\Delta L_{1,0} = 0.000, \Delta L_{1,1} = 0.512, \Delta L_{1,2} = 0.314,$ and $\Delta L_{1,3} = 0.174$. The information increments should sum to 1. This step process manifests as a gradual jump in the observed price as we saw in the methodology section.

Figure 8: A step function captures the speed with which observed prices incorporate new information



Note: This figure plots a sample path of the step function we use to contaminate an efficient jump. The efficient stock price jumps at $i\Delta_n = 11,701$ or 12:45:00. The waiting times between each of three steps are equal to $w_{1,1} = 34, w_{1,2} = 29, w_{1,3} = 49$ seconds. The sampled sizes are equal to 0.000, 0.512, 0.826, and 1.000 and the increments are equal to $\Delta L_{1,0} = 0.000, \Delta L_{1,1} = 0.512, \Delta L_{1,2} = 0.314,$ and $\Delta L_{1,3} = 0.174$.

B The vanilla rearrangement algorithm

Suppose that we want to rearrange the jump-event matrix of size $h \times q$. The rearrangement algorithm of Puccetti and Rüschendorf (2012) and Embrechts et al. (2013) loops over each column of a matrix to order it oppositely to the sum of the other columns. If the matrix has a fixed target in the last column (see *e.g.*, Bernard et al., 2018, 2017), the algorithm is as follows:

1. Randomly shuffle the elements (in each of the first $q-1$ columns) to obtain the starting matrix of the algorithm. The random shuffle flattens (*i.e.*, reduce the variability of) the row-sums.

$$J_n = \begin{bmatrix} 0.000 & 0.000 & 0.000 & -0.002 \\ 0.000 & 0.000 & 0.000 & 0.003 \\ 0.000 & 0.000 & 0.000 & -0.807 \\ \underline{0.210} & 0.000 & \underline{0.400} & 0.004 \\ 0.000 & \underline{0.217} & 0.000 & -0.028 \end{bmatrix} \xrightarrow[\text{Shuffle}]{\text{Random}} \begin{bmatrix} 0.000 & 0.000 & 0.000 & -0.002 \\ \underline{0.210} & 0.000 & 0.000 & 0.003 \\ 0.000 & 0.000 & \underline{0.400} & -0.807 \\ 0.000 & \underline{0.217} & 0.000 & 0.004 \\ 0.000 & 0.000 & 0.000 & -0.028 \end{bmatrix}$$

Weighted discontinuous stock returns
Target
Rearranged weighted discontinuous stock returns
Target

2. Iteratively rearrange the l -th column of the rearranged matrix J_n^π so that it becomes oppositely ordered to the sum of the other columns, for $l = 1, \dots, q-1$. We never rearrange the target column, $l = q$. For $l = 1$, the algorithm immediately matches the stock jump with the ETF jump:

$$\begin{bmatrix} 0.000 & 0.000 & 0.000 & -0.002 \\ \underline{0.210} & 0.000 & 0.000 & 0.003 \\ 0.000 & 0.000 & \underline{0.400} & -0.807 \\ 0.000 & \underline{0.217} & 0.000 & 0.004 \\ 0.000 & 0.000 & 0.000 & -0.028 \end{bmatrix} \xrightarrow[\text{order}]{\text{Oppositely}} \begin{bmatrix} 0.000 & 0.000 & 0.000 & -0.002 \\ 0.000 & 0.000 & 0.000 & 0.003 \\ \underline{0.210} & 0.000 & \underline{0.400} & -0.807 \\ 0.000 & \underline{0.217} & 0.000 & 0.004 \\ 0.000 & 0.000 & 0.000 & -0.028 \end{bmatrix}$$

Rearranged weighted discontinuous stock returns
Target
Rearranged weighted discontinuous stock returns
Target

3. Repeat Step 2 until no further changes occur. That is, until a matrix J_n^π is found with each column oppositely ordered to the sum of the other columns. The matrix will have row-wise sums with minimal variance.